Numerical Modelling of the plastic deformation of Ti-6Al-4V Sheets Under Explosive Loading

Dimitrios KAKOGIANNIS[1,2], Frederik COGHE[2], Luc RABET[1]

[1]Civil and Material Engineering Department, Royal Military Academy Renaissancelaan 30, B-1000, Brussels, Belgium
[2]Department of weapon systems and ballistics, Royal Military Academy Renaissancelaan 30, B-1000, Brussels, Belgium

1 Introduction

Ti-6Al-4V is the most commonly used titanium alloy (90% Ti, in weight %) in engineering applications due to its high strength, its low density and resistance to corrosion. It is an α-rich α–β Ti-alloy where the α-phase of Ti6Al4V has a hexagonal (hcp) crystal structure whereas the β-phase has a body-centered cubic (bcc) structure. Mechanical behavior of polycrystalline materials, such as Ti-6Al-4V, is linked to their texture which changes during deformation due to grain reorientations. The numerical modelling of the behavior of such material is challenging since it is highly dependent on its microstructure, exhibiting a pronounced anisotropy, strength differential and strong sensitivity to strain rate and temperature [1-3]. Crystal plasticity models have been developed to simulate the deformation of such materials, establishing a relationship between the behavior of the material and the individual grains of which it is composed. One of the polycrystalline models that has been proposed is the viscoplastic self-consistent (VPSC7) model, which has been extensively used to describe the plastic behavior, the evolution of hardening and texture, associated with plastic forming [4]. The disadvantages of such models are their complexity and high computational cost and they are not commonly used as constitutive models in full scale finite element analyses. For multiaxial loading of hcp metals, flow laws have been developed which capture both the anisotropy due to texture and the strength differential effect, such as the macroscopic orthotropic yield criterion CPB06 proposed by Cazacu et al. [5]. The CPB06 model in combination with hardening laws can describe the yield locus and its evolution, and is implemented in the commercial finite element solver LS-DYNA as **`*MAT_CAZACU_BARLAT`**/ *`MAT_233` [6]. The implementation of the model in LS-DYNA provides the possibility to fit the material parameters automatically by giving as input the yield locus stresses or to input the parameters directly.

In the present paper, starting from the texture measurement, VPSC7 is used to calculate yield stresses at high strain rates at various directions on the Ti-6Al-4V sheet. The CPB06 parameters are defined through the calculated yield stresses in two different ways: i) through the optimization method of Simulated Annealing [7] and ii) through the fitting option provided by LS-DYNA. Two finite element models (FEM) are solved in LS-DYNA calculating the response of Ti-6Al-4V sheets under explosive loading. The results from the two FEM are compared with the results of explosive forming experiments. An explosive forming setup was developed in parallel with the numerical modelling method. A shock tube is used to create a planar blast load, generated by the detonation of an explosive charge, that deforms the Ti-6Al-4V sheet specimen creating a circular dome.

2 Experimental setup and specimens

An experimental setup is designed in order to investigate the response of Ti-6Al-4V alloy sheets under explosive loading. A clamping system is created to hold a circular Ti-6Al-4V sheet. The clamping system is placed in front of a shock tube through which a planar blast wave impacts the exposed surface of the specimen. The blast load is generated by the detonation of a spherical charge of 20g of C4 placed at the beginning of the shock tube with a diameter of 150mm. The blast wave is channeled through the tube and it ends at the other side where the clamping system with the Ti-6Al-4V sheet is located. At the other end of the sheet high speed cameras are used to capture the deformation process using the Digital Image Correlation (DIC) technique to measure the in-plane strain of the sheet during deformation. The configuration is presented in Fig.1. The specimen has a diameter of 370mm and it is clamped with 10 bolts as shown in Fig.2. A torque of 20Nm is applied to all the bolts (12mm diameter) that hold the specimen. In total 6 tests are conducted: 3 specimens of 1mm and 3 specimens of 0.6mm are tested.

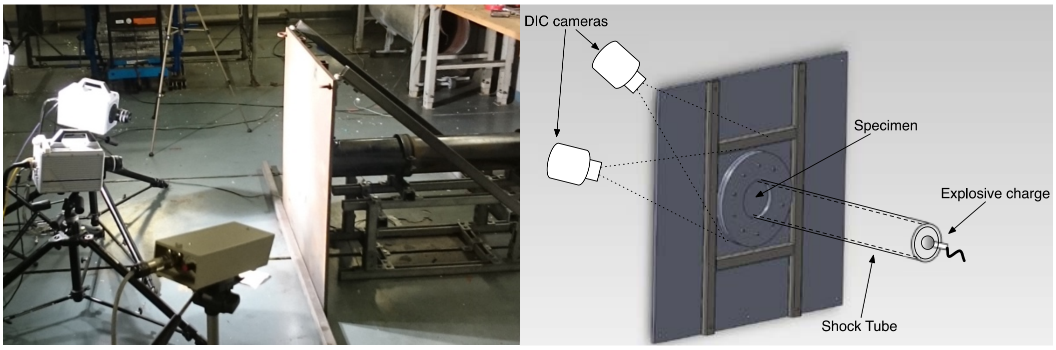

Fig.1: Left: The schematic of the setup. Right: Actual picture of the setup showing the cameras of the left and the clamping system and part of the shock tube.

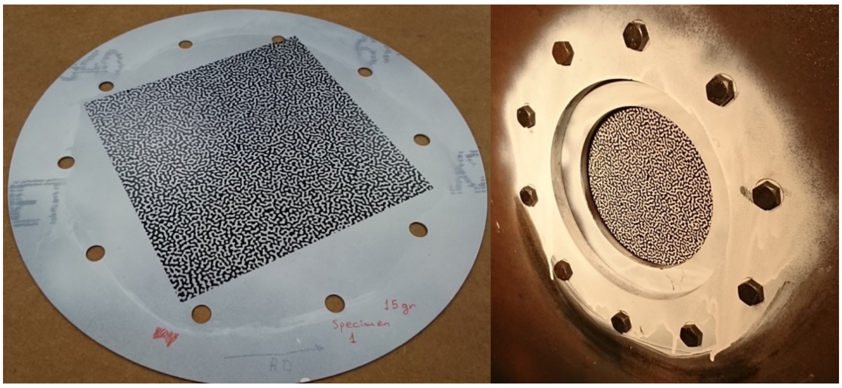

Fig.2: Left: The specimen with the speckle pattern. Right: The specimen fixed on the setup prior to testing.

3 Numerical model

The presented modelling technique relates the microstructure of the alloy with its macroscopic behavior taking into account anisotropic effects. The stress strain curves are calculated in various directions in the material through the viscoplastic self-consistent polycrystal model (VPSC7) of Lebensohn and Tomé based on the microscopic texture of the alloy. The yield stresses are used to define the parameters of the Cazacu-Barlat material model (***MAT_CAZACU_BARLAT**/ ***MAT_233**) through the optimization method of Simulated Annealing(SA) in order to define the yield locus. The method is summarized in Fig. 3.

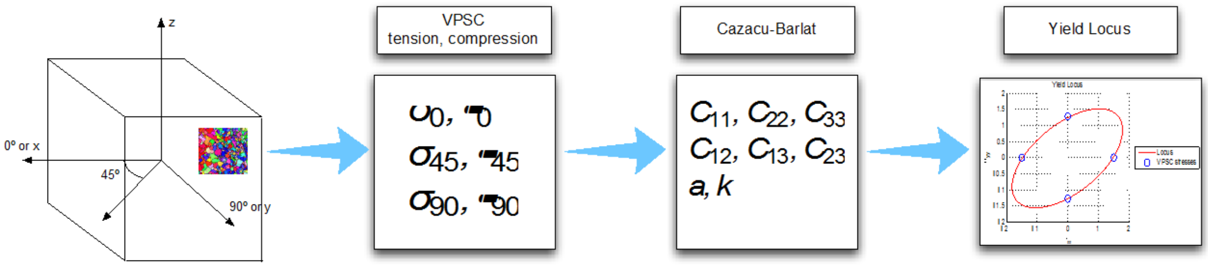

Fig.3: The steps of the modeling technique: initially the texture of the material is used as an input in the VPSC7, the yield stresses are estimated in various directions, through the yield stresses the parameters of the Cazacu-Barlat material model are estimated producing the yield locus that defines the behavior of the alloy.

3.1 Viscoplastic self-consistent polycrystal plasticity model (VPSC7)

VPSC7 is a crystal plasticity model that predicts the mechanical behavior of a polycrystal based on the behavior of each grain through the evolution of texture during deformation [4]. The model can describe the anisotropic behavior through the crystallographic texture which is correlated with the mechanical behavior of the material. The hardening curves used in the present study are calculated through the code. The model provides a link between macroscopic response and the underlying microstructure taking into account the viscoplastic deformation and neglects the elastic deformation. The results of VPSC7 are validated by quasistatic tensile tests at every 15 degrees on the sheet at a strain rate of 0.00066/s (Table1) and one tensile for a strain rate of 1000/s at the rolling direction of the sheet as illustrated in Fig.4. The VPSC7 code is used to generate the tensile and compression curves at three directions in plane at 0^o, 45^o and 90^o at a strain rate of 1000/s as summarized in Table 2.

	0°	15°	30°	45°	60°	75°	90°
Experimental yield stress(MPa)	975.73	964.7	961.03	944.3	958.3	994.3	1004.3
VPSC7 yield tress(MPa)	937.43	931.46	941.57	958.01	967.02	960.32	956.06
Relative error (%)	3.9	3.4	2.02	1.45	0.9	3.41	4.8

Table 1: Effective yield stresses of tensile tests at 0.00066/s compared with VPSC7 yield stresses.

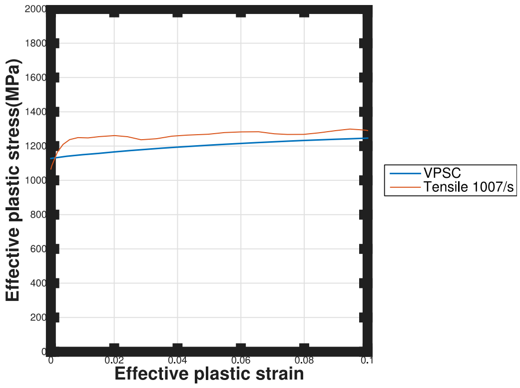

Fig.4: Validation of the VPSC7 results for a tensile test at a strain rate of 1007/s at the rolling direction.

	σ_0^t	σ_0^c	σ_{45}^t	σ_{45}^c	σ_{90}^t	σ_{90}^c	$\sigma_{biaxial}$
Yield stress (MPa)	1127.7	1127.7	1150.7	1150.7	1152.5	1152.5	1250

Table 2: Yield stresses from VPSC7 for a strain rate of 1000/s.

3.2 Cazacu-Barlat (CPB06) orthotropic yield criterion

The CPB06 model is aimed for modeling materials with strength differential and orthotropic behavior under plane stress [5]. The yield condition includes a parameter k that describes the asymmetry between yield in tension and compression. To include anisotropic behavior the stress deviator S undergoes a linear transformation and the principal values of the Cauchy stress deviator are substituted with the principal values of the transformed tensor Σ given as:

$$\Sigma = CS \tag{1}$$

in the case of a sheet the tensor C is represented by a 4x4 matrix:

$$C = \begin{bmatrix} C_{11} & C_{12} & C_{13} & \\ C_{12} & C_{22} & C_{23} & \\ C_{13} & C_{23} & C_{33} & \\ & & & C_{44} \end{bmatrix}$$

the principal values of Σ are denoted $\Sigma_1, \Sigma_2, \Sigma_3$ and are the eigenvalues of the matrix composed by the components Σ_{xx} , Σ_{yy} , Σ_{zz} , Σ_{xy} that are in function of the components of the C matrix. Finally, the orthotropic yielding criterion is given from:

$$(|\Sigma_1| - k\Sigma_1)^a + (|\Sigma_2| - k\Sigma_2)^a + (|\Sigma_3| - k\Sigma_3)^a = F \tag{2}$$

Further details about the matrix parameters can be found at Cazacu et al. [5]. The CPB06 criterion is implemented in LS-DYNA for shell elements and the parameter k and the C matrix can be either introduced by the user or they can be calculated by LS-DYNA (through **FIT** option) by providing: the yield stress in tension in 0° direction, the yield stress in compression in 0° direction, the yield stress in tension in the 45° direction, the yield stress in tension in the 90° direction and a yield stress for the balanced biaxial tension. Finally, the density, the Poisson ratio and the Young modulus need to be introduced. In the present study, the Simulated Annealing (SA) optimization method is used to estimate the parameters of the CPB06 criterion [7] by minimizing the objective function:

$$E = \sum_{i=1}^{Nd} [\frac{(VPSC7\ yield\ stress) - (numerical\ yiled\ stress)}{(VPSC7\ yield\ stress)}]^2 \tag{3}$$

The properties as calculated by the two methods are presented in Table 3.

	a	k	C_{11}	C_{22}	C_{33}	C_{12}	C_{13}	C_{23}	C_{44}
Simulated annealing (SA)	2	-0.0197	1	-1.8167	-0.3451	-3.8315	-0.3108	1.8562	3.8206
LS-DYNA fit	2	-0.680e-16	1.5802	1.5421	0.2631	0.3147	0	0	1.2278

Table 3: The estimated parameters of the Cazacu-Barlat material model.

In the implementation of the material model in LS-DYNA a hardening law is required to be used in order to define the isotropic increase of the yield locus area. In the present study, the Voce hardening law [6] is used that is described by:

$$\sigma = A - (A - B)e^{-n\varepsilon} \tag{4}$$

	A(MPa)	**B(MPa)**	**n**
Simulated annealing	4119	3432	30
LS-DYNA fit	1285	1071	30

Table 4: The values for Voce law

The parameters were calculated for a strain rate of 1000/s due to the reason that this is the maximum strain rate observed on the sheet. In Fig. 5 the yield stress in tensile versus the orientation on the sheet is plotted starting from 0° (rolling direction) to 90° (transverse direction). The yield loci from VPSC7 and the two sets of parameters from SA and LS-DYNA are presented in Fig.5.

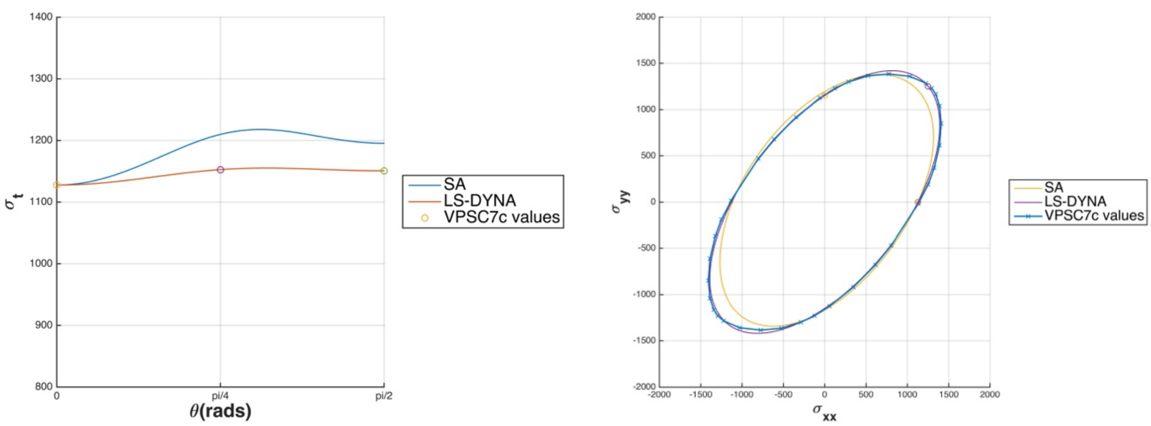

Fig.5: Left: The yield stress vs the angle for each set of parameters. Right: The yield loci occurring from the calculation of the Cazacu-Barlat parameters for a strain rate of 1000/s.

3.3 Finite element model

The section of the modelled geometry in the finite element model is shown in Fig. 6. The model consists of three parts: the top plate, the specimen and the die on which the top plate is fixed. In the finite element model the bolds are omitted and a boundary condition is applied that allows to the specimen to slide at the bolt holes but is fixed in the area of contact with the bolts during deformation. The contact algorithm ***AUTOMATIC_ONE_WAY_SURFACE_TO_SURFACE** [6] is used to simulate the contact between the specimen, the top plate and the die. The material properties of Tables 3 and 4 are used in ***MAT_CAZACU_BARLAT**. The experimental pressure of the blast wave is applied through the function:

$$\begin{aligned} P(r) &= P_o \, for \; 0 \le r \le r_o \\ P(r) &= P_o e^{-0.2(r-r_o)} \, for \; r_o \le r \le r_{surf} \end{aligned} \tag{5}$$

where P_o is the peak pressure, r is the radius of the planar wave, r_o is the radius of the shock tube and r_{surf} is the radius of the surface on which the blast wave is applied (see Fig.7).

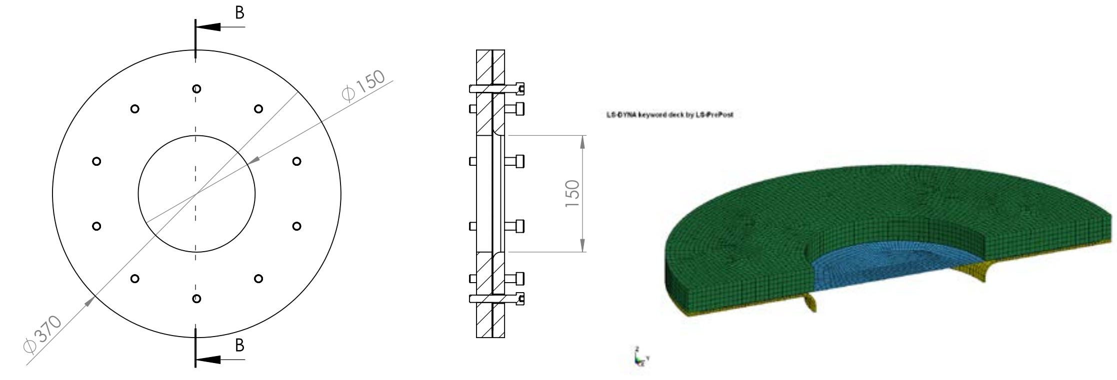

Fig.6: Left: the schematic of the specimen and the clamping system. Right: the section of the finite element model.

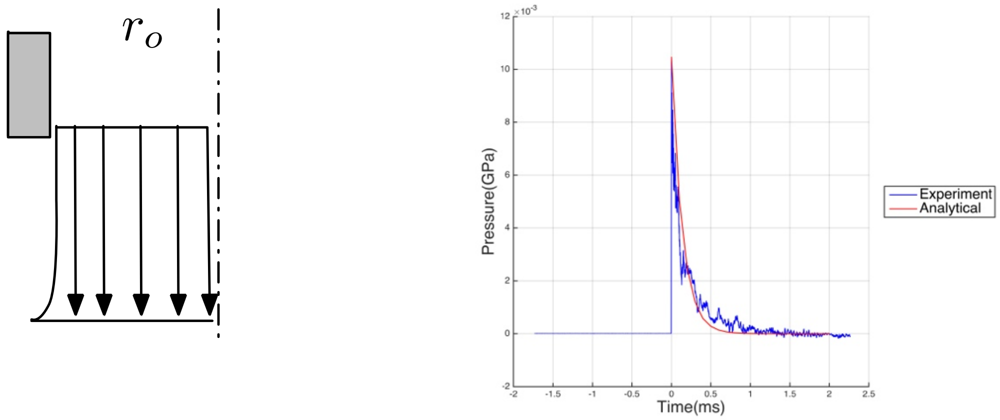

Fig.7: Left: the schematic of the pressure on the sheet. Right: the signal of reflected pressure on the plate.

4 Results

The results of displacement and maximum strain at the rolling direction of the sheet are presented in Fig. 8 where a comparison is made with the numerical values. The results produced by the model in which the parameters of CPB06 criterion are calculated from SA are closer to the experimental values for both thicknesses. The deviation of numerical results could be attributed to the reason that the numerical model properties are homogeneously applied to the whole area of the specimen assuming strain rate of 1000/s, which is the maximum strain rate measured experimentally in the centre of the specimen. An overview of the profiles of the experimental and numerical displacement are presented in Fig. 9, along the rolling direction of the sheet. The displacement of the 1mm sheet where LS-DYNA calculates the C matrix for the model shows an irregular deformation where the mid-point “locks” in a position creating a rippling effect on the sheet.

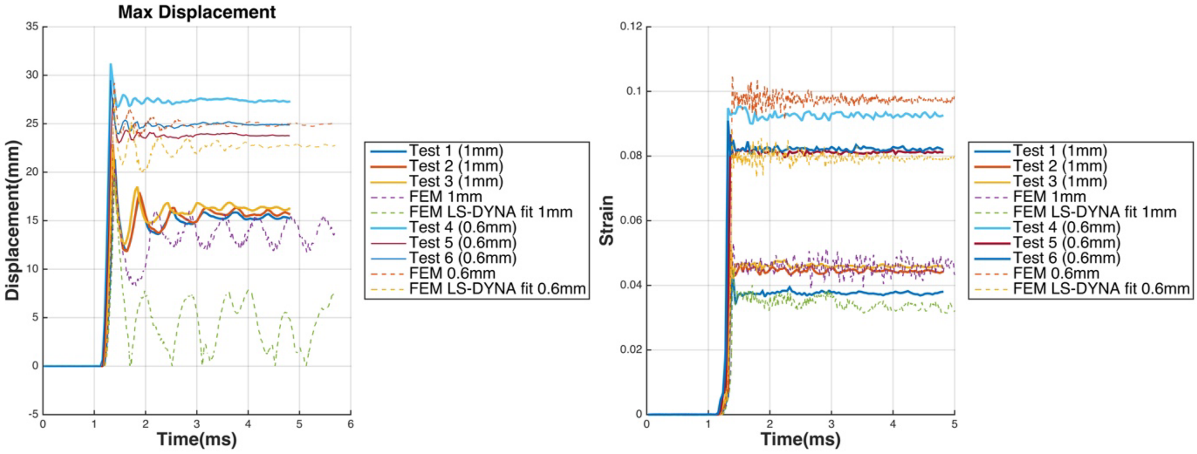

Fig.8: Left: comparison of the maximum displacement at the centre of the plate vs. time. Right: comparison of the strains at the rolling direction of the plate vs. time.

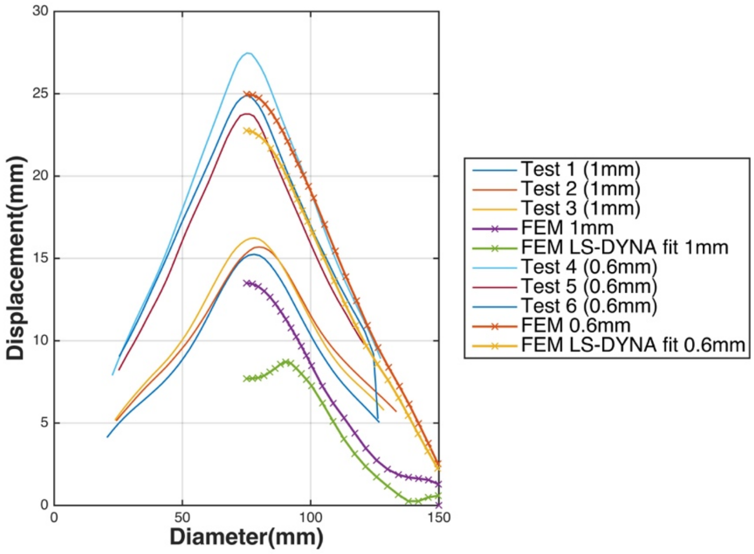

Fig.9: The profiles of the final displacements of the plates of all the tests in comparison with the FEM results.

Anisotropy can be observed by the contours of displacement, for the 1mm sheet that oscillates the most, as seen in Fig. 10. As illustrated, during oscillation certain eigenmodes of the sheet reveal the anisotropy at the various directions in the material. These oscillations are also observed in the finite element model for the same thickness, since the purpose of the chosen material model is to model anisotropy during plastic deformation. As It can be observed, the SA FEM model produces similar contours to the experimental. The contours of the LS-DYNA fitting option produce irregular patters on displacement at all directions.

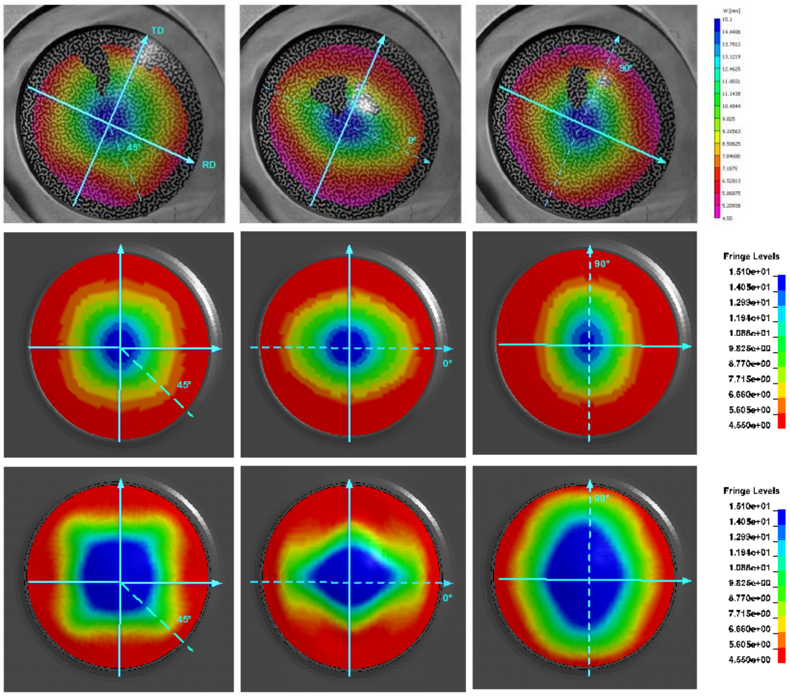

Fig.10: Top to bottom: The experimental contours of displacement for 1mm sheets, the SA FEM contours and the LS-DYNA fitting contours. During vibration in certain eigenmodes the patterns of the dome have an elliptic shape as seen in the picture for 0^o,45^o and 90^o.

5 Summary

A multi-scale modelling method is presented for predicting the response of Ti-6Al-4V sheets under explosive loading, evaluated by experiments. Starting from texture measurements, the stress-strain curves of the crystal plasticity model VPSC7 are validated by experiments under quasistatic strain rate. Based on VPSC7 to calculate the yield stresses at dynamic strain rate, the parameters of the macroscopic material model **`*MAT_CAZACU_BARLAT`**/ **`*MAT_233`** are defined by two different methods. The estimated parameters of the two methods are used to create two finite element models to predict the plastic deformation of sheets under explosive loading and evaluate them by comparing with experiments.

The presented method allows by a set of experiments at low strain rates to estimate the yield stresses and the yield locus of the material for dynamic rates without an extensive experimental campaign. The CBP06 criterion and its implementation in LS-DYNA gives the possibility to predict the plastic deformation of Ti-6Al-4V sheets, in combination with anisotropy, under complex biaxial loads at high strain rates as presented. Attention is required by the user when estimating the parameters of the model because the similar loci can produce significantly different plastic deformations. As observed in the results, the fitting option, provided by LS-DYNA, requires further investigation. Nodal displacement should be used in combination with strain measurements considering the differences observed between numerical and experimental results in order to decide on the accuracy of the model and its parameters. The differences between numerical and experimental results can be attributed to the fact that the calculated yield locus of 1000/s is applied on all the elements of the sheet. In reality the maximum strain rate is on the center of the specimen and it reduces radially towards the edge of the clamping system. A future improvement could be the separation of the sheet into concentric zones of strain rates that correspond to the rates measured at the same points on the specimen.

The authors gratefully acknowledge the financial support provided by the Belgian Science Policy Office (BELSPO), INTEMATE P7/21.

6 Literature

[1] Galán, J., Verleysen, P. and Degrieck, J., “Thermal effects during tensile deformation of Ti-6Al-4V at different strain rates”, *Strain*, Vol. 49, 2013, pp. 354-365.

[2] Peirs, J., Verleysen, P., Van Paepegem, W. and Degrieck, J. “Determining the stress-strain behaviour at large strains from high strain rate tensile and shear experiments”, *International Journal of Impact Engineering*, Vol. 38, 2011, pp. 406-415.

[3] Gilles, G., Hammami, W., Libertiaux, V., Cazacu, O., Yoon, J.H., Kuwabara, T. and Hebraken, A.M., “Experimental characterization and elastoplastic modelling of the quasistatc mechanical response of TA-6V at room temperature”, *International Journal of Solids and Structures*, Vol. 48, 2011, pp. 1277-1289.

[4] Lebensohn, R. A. and Tomé, C. N., “A self-consistent anisotropic approach for the simulation of plastic deformation and texture development of poly crystals: application to zirconium alloys”, *Acta Metallurgica et Materialia*, Vol. 43, 1993, pp. 2611-2624.

[5] Cazacu O., Plunkett B., Barlat F., “Orthotropic yield criterion for hexagonal closed packed metals”, *International Journal of Plasticity*, 22(7), 2006, pp. 1171-1194.

[6] Halquist J., “LS-DYNA keyword user’s manual version 971”, *Livermore Software Technology Corporation*, Livermore, CA, 2007.

[7] Gilles G., Habraken A. M., Duchene L., “Material Parameter Identification of Cazacu’s Model for Ti6Al4V Using the Simulated Annealing Algorithm”, *In Materials Science Forum, Trans Tech Publications*, Vol. 636, 2010, pp. 1125-1130.